

# Incorporation of Fluorotyrosines into Ribonucleotide Reductase Using an Evolved, Polyspecific Aminoacyl-tRNA Synthetase

Ellen C. Minnihán,<sup>†,||</sup> Douglas D. Young,<sup>§,||</sup> Peter G. Schultz,<sup>\*,§</sup> and JoAnne Stubbe<sup>\*,†,‡</sup>

<sup>†</sup>Department of Chemistry and <sup>‡</sup>Department of Biology, Massachusetts Institute of Technology, 77 Massachusetts Avenue, Cambridge, Massachusetts 02139, United States

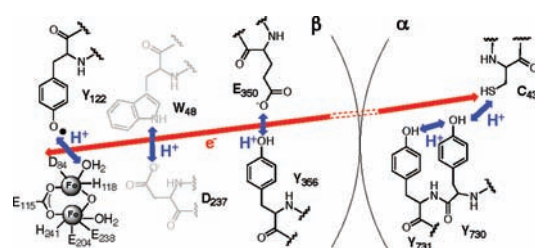
<sup>§</sup>Department of Chemistry, The Scripps Research Institute, 10550 North Torrey Pines Road, La Jolla, California 92037, United States

**S** Supporting Information

**ABSTRACT:** Tyrosyl radicals ( $Y\cdot$ s) are prevalent in biological catalysis and are formed under physiological conditions by the coupled loss of both a proton and an electron. Fluorotyrosines ( $F_nY$ s,  $n = 1-4$ ) are promising tools for studying the mechanism of  $Y\cdot$  formation and reactivity, as their  $pK_a$  values and peak potentials span four units and 300 mV, respectively, between pH 6 and 10. In this manuscript, we present the directed evolution of aminoacyl-tRNA synthetases (aaRSs) for 2,3,5-trifluorotyrosine (2,3,5- $F_3Y$ ) and demonstrate their ability to charge an orthogonal tRNA with a series of  $F_nY$ s while maintaining high specificity over  $Y$ . An evolved aaRS is then used to incorporate  $F_nY$ s site-specifically into the two subunits ( $\alpha 2$  and  $\beta 2$ ) of *Escherichia coli* class Ia ribonucleotide reductase (RNR), an enzyme that employs stable and transient  $Y\cdot$ s to mediate long-range, reversible radical hopping during catalysis. Each of four conserved  $Y$ s in RNR is replaced with  $F_nY$ (s), and the resulting proteins are isolated in good yields.  $F_nY$ s incorporated at position 122 of  $\beta 2$ , the site of a stable  $Y\cdot$  in wild-type RNR, generate long-lived  $F_nY\cdot$ s that are characterized by electron paramagnetic resonance (EPR) spectroscopy. Furthermore, we demonstrate that the radical pathway in the mutant  $Y_{122}(2,3,5)F_3Y\text{-}\beta 2$  is energetically and/or conformationally modulated in such a way that the enzyme retains its activity but a new on-pathway  $Y\cdot$  can accumulate. The distinct EPR properties of the 2,3,5- $F_3Y\cdot$  facilitate spectral subtractions that make detection and identification of new  $Y\cdot$ s straightforward.

Examples of amino acid radicals participating in charge-transfer reactions are prevalent in nature.<sup>1</sup> Of these, tyrosyl radicals ( $Y\cdot$ s) have been shown to mediate a number of key metabolic transformations, including  $O_2$  evolution, fatty acid oxidation, peroxide disproportionation, and prostaglandin synthesis.<sup>2</sup> The thermodynamics of  $Y$  oxidation require that proton transfer (PT) accompanies electron transfer (ET) at physiological pH, a process that may occur by either a stepwise or coupled (PCET) mechanism. To investigate the mechanism of  $Y\cdot$  formation and  $Y\cdot$ -mediated catalysis in metalloenzymes, a method by which the native  $Y\cdot$  may be subtly perturbed is needed. A series of *N*-acetylfluorotyrosinamides (*N*-Ac- $F_nY\text{-NH}_2$ s) were characterized in solution and found to have phenolic  $pK_a$  values ranging from 5.6 to 8.4 and peak potentials ranging from 705 to 968 mV.<sup>3,4</sup> This series of  $Y$  analogues provides a means of systematically modulating the chemical properties governing both the PT and ET events.

**Scheme 1. Working Mechanism for the Long-Range PCET Pathway in *E. coli* Class Ia RNR<sup>a</sup>**



<sup>a</sup>The current hypothesis holds that protons (blue arrows) move orthogonally to the electron (red arrow) in  $\beta 2$  and co-linearly with the electron in  $\alpha 2$ . The mechanism across the  $\alpha/\beta$  interface is unknown. There is no direct evidence that  $W_{48}$  and its putative  $H^+$  acceptor,  $D_{237}$ , participate in long-range PCET during turnover.

Ribonucleotide reductase (RNR) catalyzes the formation of all four 2'-deoxynucleotides from the corresponding nucleoside diphosphates (NDPs) by a mechanism involving protein and nucleotide radicals.<sup>1</sup> In the class Ia RNRs, a stable diferric- $Y\cdot$  cofactor in the  $\beta 2$  subunit initiates catalysis by transiently oxidizing a cysteine at the active site in the  $\alpha 2$  subunit. The mechanism of radical initiation has been best studied in *Escherichia coli* RNR and is believed to involve an unprecedented mechanism of reversible long-range ( $>35$  Å) PCET along a pathway of absolutely conserved redox-active amino acids:  $Y_{122}\cdot \leftrightarrow [W_{48}^{\cdot}] \leftrightarrow Y_{356}$  in  $\beta 2$  to  $Y_{731} \leftrightarrow Y_{730} \leftrightarrow C_{439}$  in  $\alpha 2$  (Scheme 1).<sup>5,6</sup> This hypothesis has been tested by the site-specific incorporation of more than a half-dozen unnatural amino acids (UAAs) at positions along the pathway using both expressed protein ligation (EPL)<sup>7</sup> and in vivo nonsense suppression<sup>8,9</sup> techniques. Studies in which a series of fluorotyrosines ( $F_nY$ s) were incorporated at position 356 of  $\beta 2$  by EPL were particularly informative, as the pH rate profiles of the resulting proteins indicated that this residue is redox-active, that proton and electron movement is orthogonal at this position (Scheme 1), and that an ordered H-bonding network involving the  $Y_{356}$  phenol is not necessary for catalysis.<sup>10,11</sup>

$F_nY$ s incorporated in place of other conserved  $Y$ s along the pathway would be comparably informative. However, the EPL technology used to generate  $Y_{356}F_nY\text{-}\beta 2$ s cannot be readily extended to positions in the protein interior. While other strategies

Received: August 15, 2011

Published: September 13, 2011

for incorporation of  $F_nY$ s exist, namely, global incorporation<sup>4,12</sup> or site-specific insertion of photocaged  $F_nY$ s,<sup>13</sup> these techniques are applicable to mono- and di- $F_nY$ s only and are minimally useful in RNR, as the former lacks specificity and the latter leads to complications arising from photolysis.<sup>14</sup>

Herein, a robust method for in vivo site-specific incorporation of a series of  $F_nY$ s is reported. This method requires evolution of an orthogonal aminoacyl-tRNA synthetase (aaRS)–tRNA pair and has been successfully used to incorporate over 70 UAAs into *E. coli*, *Saccharomyces cerevisiae*, and mammalian proteins in response to a nonsense (or “blank”) codon.<sup>15,16</sup> Originally, we sought to evolve an aaRS specific for 2,3,5-trifluorotyrosine (2,3,5- $F_3Y$ , **1**), as previous data suggested that its redox potential is sufficiently increased relative to Y at appropriate pHs that its incorporation at position 356 of  $\beta 2$  changes the rate-determining step in RNR from a conformational change<sup>17</sup> to PCET.<sup>11</sup> Three fluorine substituents together with the low phenolic  $pK_a$  (6.4) were expected to allow the evolution of an RS selective for the phenolate of **1** over the Y phenol.

To incorporate **1** into proteins selectively, an orthogonal *Methanococcus jannaschii* aaRS–tRNA pair that suppresses the amber stop codon (TAG) was evolved to encode this amino acid uniquely by a double-sieve selection process based on cellular viability.<sup>16</sup> A library of TyrRS mutants was generated by randomizing eight positions near the active site based on the known structure of Tyr-bound *Mj*TyrRS,<sup>18</sup> including those residues closest to the aromatic ring (Y32, L65, and H70) and those involved in H-bonding to the Y phenol (Y32 and D158). The library was subjected to three positive and negative selection cycles, after which individual candidates were isolated and assessed for viability in the presence and absence of **1** at different chloramphenicol (*Cm*) concentrations. The selection resulted in two primary clones, E3 (Y32L, L65G, H70N, F108F, Q109Q, D158S, I159Y, L162H) and E11 (Y32H, L65Y, H70G, F108Y, Q109A, D158N, I159I, L162R), that conferred *Cm* resistance (>150  $\mu\text{g}/\text{mL}$ ) only in the presence of **1** (Figure S1 and Table S1 in the Supporting Information). Given the mutations and the structure,<sup>18</sup> we tried to understand the basis for recognition of **1** by the aaRSs (Figure S2). We had predicted that the negative charge on the phenolate of **1** would be the basis for discrimination against Y and anticipated the introduction of positively charged side chains in the mutants. E3 contains a L162H mutation, but the protonation state of this residue is unknown. E11 contains a single basic side chain (L162R); however, a crystal structure of the *p*-acetylphenylalanine RS containing the same mutation revealed that the R side chain was directed away from the active site.<sup>19</sup> Y32 and/or D158 are mutated in both 2,3,5- $F_3Y$ -RSs to residues that could conceivably behave as H-bond donors to the phenolate of **1**. The substitution of Gly at either position 65 (E3) or 70 (E11) may enlarge the substrate binding pocket. Thus, there exists minimal evidence indicating that the observed discrimination occurs on the basis of the phenolate. Instead, it appears that the fluorine substituents provide the key recognition elements. The introduction and retention of many polar side chains provide opportunities for the three F atoms to participate in multipolar interactions of the nature  $C-F\cdots H-N/O$  or  $C-F\cdots C=O$ .<sup>20</sup> In view of the sensitivity of these interactions to distance and geometry, it is impossible to speculate on the specific atoms involved without a high-resolution structure. Crystallization attempts to provide a better understanding of the basis of F–protein interactions in the 2,3,5- $F_3Y$ -RSs are underway. The nature of these interactions

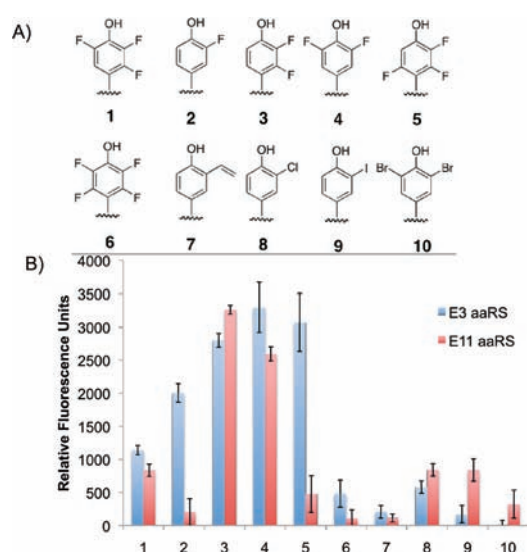


**Figure 1.** Polyspecificity of  $F_nY$ -RSs. (A) Y analogues that screened positive for GFP incorporation. (B) GFP fluorescence assay of the two evolved aaRSs (blue, E3; red, E11) based on suppression of GFP<sub>Y151TAG</sub> in the presence of 1 mM UAA.

is of general interest, given the large number of fluorinated pharmaceuticals.<sup>20</sup>

The aaRS hits were cloned into the previously described pEVOL system<sup>21</sup> for enhanced expression of proteins containing **1**. We confirmed the selective incorporation of **1** into proteins by aaRSs E3 and E11 using pET-GFP<sub>Y151TAG</sub>, a plasmid that encodes a C-terminally His<sub>6</sub>-tagged green fluorescent protein (GFP).<sup>15</sup> Full-length fluorescent protein is observed only when the TAG codon is suppressed by an amino-acylated tRNA. E3 afforded 10 mg/L of purified GFP, while E11 yielded 4 mg/L. Both aaRSs incorporated **1** into GFP with an observed mass of 27 759 Da (27 758 Da expected; see Figure S3). In the absence of **1**, low levels of phenylalanine incorporation could be detected for E3; however, this background incorporation was not detected in the presence of **1** (a property observed with several previously evolved aaRSs).<sup>22a</sup> No background incorporation was detected for E11 in the absence of **1**.

Recent experiments have shown that some aaRSs exhibit a degree of polyspecificity.<sup>22</sup> This feature arises from the lack of other UAAs in the selection medium to eliminate synthetases that can recognize them. To determine whether these 2,3,5- $F_3Y$  aaRSs are polyspecific, they were screened against a diverse library of UAAs using a GFP fluorescence assay.<sup>22a</sup> Of the ~80 UAAs in the library, both aaRSs were capable of aminoacylating 3-fluorotyrosine (**2**) and 3-chlorotyrosine (**8**) (Figure S4). The results of this first screen indicated that the aaRSs exhibit some polyspecificity for other halogenated Ys, prompting a second GFP screen on Ys with a narrower range of substitutions (including **3–7**, **9**, and **10**). The evolved aaRSs were capable of incorporating all members of the  $F_nY$  series [3-FY (**2**), 2,3- $F_2Y$  (**3**), 3,5- $F_2Y$  (**4**), 2,3,6- $F_3Y$  (**5**), and 2,3,5,6- $F_4Y$  (**6**)] as well as several other halogenated analogues (Figure 1). The incorporation of each UAA was confirmed by LC/MS analysis of the mutant GFPs (Figure S5). Interestingly, several of the analogues (**2–5**) were incorporated into GFP at higher levels than **1**, thus the evolved aaRSs are henceforth called “ $F_nY$ -RSs.” LC/MS analysis of *E. coli* lysate indicated that reduced cellular uptake is one reason for the low incorporation of **6** relative to the other  $F_nY$ s.

The  $F_nY$ -RS E3 was then used to incorporate  $F_nY$ s at positions 730 and 731 of the RNR  $\alpha 2$  subunit (Scheme 1). These residues were recently shown to be sites of transient  $Y\cdot$  formation during radical propagation by substitution of 3-aminotyrosine ( $NH_2Y$ )<sup>8</sup> and 3-nitrotyrosine ( $NO_2Y$ )<sup>9</sup> at these positions using similar technology. Cells were transformed with pEVOL- $F_nY$ -RS-E3 and pET- $nrdA_{Y730TAG}$ , encoding for  $\alpha$  with a N-His<sub>6</sub> tag and a stop codon at the position of  $Y_{730}$ ,<sup>23</sup> and grown in the presence of **1**. SDS-PAGE of whole cells after induction revealed a  $\sim 1:1$  ratio of full-length and truncated proteins (Figure S6). The desired protein,  $Y_{730}(2,3,5)F_3Y\text{-}\alpha 2$ , was isolated by Ni-NTA chromatography to give 10 mg of protein/g of cell paste ( $\sim 50$  mg/L of culture). An analogous protocol was used to incorporate **3**, **4**, and **5** at position 730 of  $\alpha 2$ . These  $Y_{730}F_nY\text{-}\alpha 2$ s were purified in yields of 2.5–3 mg/g (Table S2). Consistent with the GFP data (Figure 1), the yield of protein containing **6** was 10-fold lower than for the other  $F_nY$ s. The 730-optimized protocol was then used to incorporate **1** and **4** at position 731 of  $\alpha 2$  with comparable protein yields. Finally, the expression protocol was used with minor modification to incorporate **1** at position 356 of  $\beta 2$ , and the protein was purified (2 mg/g).

Incorporation of  $F_nY$ s at position 122 of  $\beta 2$ , the site of the stable  $Y\cdot$  ( $t_{1/2} \approx 4$  days, 4 °C) in the wild type (wt), was of mechanistic interest. The reduction of  $Y_{122}\cdot$  occurs concomitant with oxidation of  $C_{439}$  in  $\alpha 2$  (Scheme 1), yet the intermediates of radical propagation in the wt enzyme are kinetically masked by rate-limiting conformational changes.<sup>17</sup> Thus, changes to  $Y_{122}\cdot$  or any of the pathway residues are undetectable by rapid biophysical techniques. Furthermore, even in those mutant RNRs in which radicals can be trapped and/or conformational gating can be partially lifted, observation and identification of new radicals by X-band EPR spectroscopy is complicated by their extensive spectral overlap. Recently, site-specific insertion of  $NO_2Y$  at position 122 of  $\beta 2$  was described. Reaction of apo- $Y_{122}NO_2Y\text{-}\beta 2$  with  $Fe^{2+}$  and  $O_2$  led to the assembly of a diferric- $NO_2Y_{122}\cdot$  cluster.<sup>24</sup> Use of the potent oxidant  $NO_2Y_{122}\cdot$  as a radical initiator decoupled the ET from the rate-limiting conformational change and allowed the first detection of a transient  $Y\cdot$  on the pathway.<sup>24,25</sup> However, the high redox potential of  $NO_2Y$  relative to  $Y$  ( $\Delta \approx 200$  mV, pH 7) introduced complications into the system, namely, the short half-life of  $NO_2Y_{122}\cdot$  ( $t_{1/2} \approx 40$  s, 25 °C) and the mutant's inability to perform multiple turnovers.

Given these results, we sought to modulate the properties of position 122 more subtly using  $F_nY$ s. In view of the known perturbation of the phenolic  $pK_a$  at this position ( $>2.5$  units),<sup>9</sup> UAAs **1** and **4** should be protonated at physiological pH and are predicted to be  $<10$  mV harder and  $\sim 50$  mV easier to oxidize than  $Y\cdot$ , respectively. Using pEVOL- $F_nY$ -RS-E3 and pBAD- $nrdB_{Y122TAG}$ , encoding untagged  $\beta 2$  with a stop codon at position 122,<sup>24</sup> the proteins  $Y_{122}(2,3,5)F_3Y\text{-}\beta 2$  and  $Y_{122}(3,5)F_2Y\text{-}\beta 2$  were expressed and isolated by anion-exchange chromatography in yields of  $\geq 30$  mg/g. The two mutants were characterized by UV-vis and EPR spectroscopy to determine whether they contained any  $F_nY\cdot$ . The as-isolated wt subunit contains 1.2  $Y\cdot/\beta 2$ , with a sharp diagnostic absorbance at 411 nm and a doublet X-band EPR spectrum dominated by coupling to one of the  $\beta$ -methylene protons (Figure 2, black). As-isolated  $Y_{122}(3,5)F_2Y\text{-}\beta 2$  and  $Y_{122}(2,3,5)F_3Y\text{-}\alpha 2$  had absorptions at  $\lambda_{max} = 396$  and 404 nm, respectively, consistent with the values determined for 3,5- $F_2Y\cdot$  and 2,3,5- $F_3Y\cdot$  generated by photooxidation of benzophenone- $F_nY$ -OMe dipeptides.<sup>4</sup>

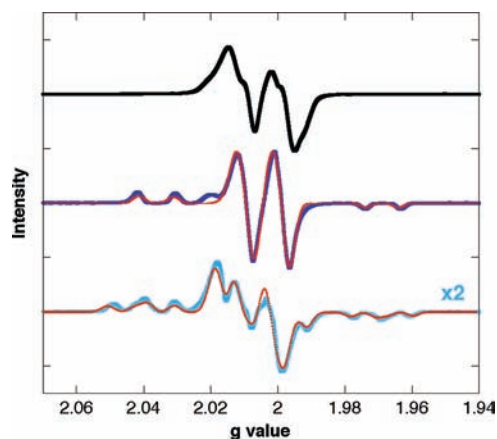


**Figure 2.** X-band EPR spectra of *E. coli* wt  $Y_{122}\cdot$  (black), 3,5- $F_2Y_{122}\cdot$  (dark blue), and 2,3,5- $F_3Y\cdot$  (cyan). Spectra were recorded at 77 K and normalized for radical concentration. Simulations (red) were performed using EasySpin.<sup>26</sup>

X-band EPR analysis of the purified proteins at 77 K indicated that the as-isolated 3,5- $F_2Y$  and 2,3,5- $F_3Y$  mutants contained 0.2 and 0.02  $F_nY_{122}\cdot/\beta 2$ , suggesting that the  $F_nY_{122}\cdot$ s are inherently less stable than native  $Y_{122}\cdot$ . Higher radical content was obtained for 2,3,5- $F_3Y_{122}$  mutants (0.4–0.9 2,3,5- $F_3Y_{122}\cdot/\beta 2$ ) by in vitro reconstitution of the cofactor.<sup>27</sup> Both the 3,5- $F_2Y_{122}\cdot$  and the 2,3,5- $F_3Y_{122}\cdot$  were stable for more than 30 min at 4 °C. The EPR spectra of the putative 3,5- $F_2Y\cdot$  and 2,3,5- $F_3Y\cdot$  at position 122 of  $\beta 2$  (Figure 2, blue and cyan) are quite distinct from those of  $F_nY\cdot$ s generated on the corresponding free amino acids by UV photolysis.<sup>4</sup> The spectra of the latter are relatively featureless, with line broadening arising from a large distribution of dihedral angles for the  $\beta$ -methylene protons. In contrast, structural constraints imposed by the protein give rise to  $F_nY_{122}\cdot$  spectra with well-defined couplings to the fluorine nuclei (150–180 MHz) and one of the  $\beta$ -methylene protons (36–48 MHz). Spectral simulations (Figure 2, red; Table S3) were conducted using the parameters for 3- $FY_{122}\cdot$  as an initial reference.<sup>4</sup> High-field EPR/ENDOR analysis of the  $F_nY\cdot$ s is ongoing (Myers, Minnihan, Stubbe, and Britt).

Nucleotide reductase assays of  $Y_{122}(2,3,5)F_3Y\text{-}\beta 2$  revealed the mutant has 30% of the wt  $\beta 2$  activity (scaled for radical). This result suggests that introduction of 2,3,5- $F_3Y$  at position 122 slightly perturbs the radical propagation energetics and/or the conformational changes that gate it, but not to the extent that it prevents multiple catalytic turnovers. The reactivity of this mutant was further investigated by EPR spectroscopy.  $Y_{122}(2,3,5)F_3Y\text{-}\beta 2$  was mixed on ice with wt- $\alpha 2$ , CDP (substrate), and ATP (allosteric effector) under single-turnover conditions in an EPR tube and quenched in a dry ice/acetone bath at 20 s. The spectrum of the reaction mixture (Figure 3, black) is a composite of the spectra of two species: 2,3,5- $F_3Y_{122}\cdot$  (pink) and a new radical (blue). Subtraction of the former from the composite was done using the fluorine hyperfine couplings, which occur in unobstructed regions of the spectrum. Calculation of the double integral intensities of the two species indicated that the new radical constitutes 25% of the total spin. The new radical is assigned as  $Y_{356}\cdot$  on the basis of additional EPR experiments in which the pathway was blocked at specific positions by insertion of a redox-inert F. Indeed, when  $Y_{122}(2,3,5)F_3Y\text{-}\beta 2$  was reacted with  $Y_{731}F\text{-}\alpha 2$ , a very similar new radical was formed in identical yield (Figure S7). A reaction with the double mutant  $Y_{122}(2,3,5)F_3Y/Y_{356}F\text{-}\beta 2$  and wt- $\alpha 2$  gave no evidence of a new radical. The assignment was further substantiated by the strong similarity of this radical to the

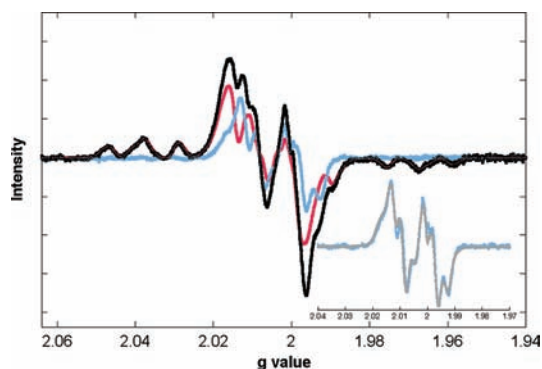


**Figure 3.** EPR spectrum of the reaction of  $Y_{122}(2,3,5)F_3Y\text{-}\beta 2$ , wt- $\alpha 2$ , CDP, and ATP quenched at 20 s. Subtraction of the  $2,3,5\text{-}F_3Y_{122}\cdot$  contribution (pink) from the reaction spectrum (black) gives a new radical (blue). Inset: overlay of the new radical with  $Y_{356}\cdot$  formed by  $Y_{122}NO_2Y\text{-}\beta 2$  (gray).

one observed when  $NO_2Y_{122}\cdot$  was used as a radical initiator (Figure 3 inset).<sup>24</sup> Extensive evidence suggests that the new radical in the  $NO_2Y$  mutant is primarily located at  $Y_{356}$ .<sup>25</sup>

While it is necessary to determine the kinetic competence of the new radical, observation of a putative  $Y_{356}\cdot$  is promising in two regards. First, the ability to observe an on-pathway  $Y\cdot$  (while maintaining significant catalytic activity) will have important mechanistic implications. Investigations to determine what properties of  $F_3Y$  allow observation of this new radical are underway. We anticipate deriving additional insight into the long-range PCET mechanism by modulating the driving force and phenolic  $pK_a$  at positions on the pathway in a stepwise fashion. Similarly,  $F_nY$ s may be utilized for mechanistic studies of ET and/or PT in model proteins and native enzymes.

Additionally, this result demonstrates the utility of  $F_nY\cdot$  as spectroscopic handles. The width of the  $F_nY\cdot$  X-band EPR spectra and the presence of distinct fluorine hyperfine couplings, which give rise to features in the low- and high-field spectral regions, allow accurate subtraction of  $F_nY\cdot$ s from other  $g \approx 2$  radicals (e.g.,  $Y\cdot$ ,  $[\beta\text{-}^2H_2]Y\cdot$ ,  $NH_2Y\cdot$ ,  $NO_2Y\cdot$ ).<sup>8,24</sup> Thus,  $F_nY\cdot$ s afford the first opportunity to identify low concentrations of radical species that would otherwise go undetected in complicated reaction mixtures.<sup>25</sup>  $F_nY\cdot$ s may prove similarly useful in high-field EPR and ENDOR studies. For proteins that do not use radicals,  $F_nY$ s may be incorporated as probes of structure and/or local environment for  $^{19}F$  NMR studies.<sup>28</sup> Thus, the application of  $F_nY$ s as spectroscopic probes may be extended to a broad biophysical research community.

## ■ ASSOCIATED CONTENT

**Supporting Information.** Methods;  $F_nY$ -RS selection; structure of  $MjTyrRS$  active site; GFP polyspecificity screen; LC/MS of  $F_nY$ -GFPs; expression/purification of  $F_nY$ -RNRS; EPR reaction spectra for  $Y_{122}(2,3,5)F_3Y\text{-}\beta 2$  with blocked mutants. This material is available free of charge via the Internet at <http://pubs.acs.org>.

## ■ AUTHOR INFORMATION

### Corresponding Author

[schultz@scripps.edu](mailto:schultz@scripps.edu); [stubbe@mit.edu](mailto:stubbe@mit.edu)

### Author Contributions

<sup>||</sup>These authors contributed equally.

## ■ ACKNOWLEDGMENT

This work was supported by NIH Grant GM29595 (J.S.) and Grant DE-FG03-00ER46051 from the Division of Materials Sciences,

Department of Energy (P.G.S.). D.D.Y. acknowledges an NIH Ruth L. Kirchstein Postdoctoral Fellowship (F32CA144213). We thank the Gao Lab (Boston College) for providing Fmoc- $F_4Y$ .

## ■ REFERENCES

- (1) Stubbe, J.; van der Donk, W. A. *Chem. Rev.* **1998**, *98*, 705.
- (2) (a) Barry, B. A.; el-Deeb, M. K.; Sandusky, P. O.; Babcock, G. T. *J. Biol. Chem.* **1990**, *265*, 20139. (b) Gupta, A.; Mukherjee, A.; Matsui, K.; Roth, J. P. *J. Am. Chem. Soc.* **2008**, *130*, 11274. (c) Zhao, X.; Suarez, J.; Khajao, A.; Yu, S.; Metlitsky, L.; Magliozzo, R. S. *J. Am. Chem. Soc.* **2010**, *132*, 8268.
- (d) Tsai, A. L.; Kulmacz, R. J. *Arch. Biochem. Biophys.* **2010**, *493*, 103.
- (3) Kim, K.; Cole, P. A. *J. Am. Chem. Soc.* **1998**, *120*, 6851.
- (4) Seyedsayamdost, M. R.; Reece, S. Y.; Nocera, D. G.; Stubbe, J. *J. Am. Chem. Soc.* **2006**, *128*, 1569.
- (5) Uhlin, U.; Eklund, H. *Nature* **1994**, *370*, 533.
- (6) Stubbe, J.; Nocera, D. G.; Yee, C. S.; Chang, M. C. Y. *Chem. Rev.* **2003**, *103*, 2167.
- (7) (a) Yee, C. S.; Seyedsayamdost, M. R.; Chang, M. C. Y.; Nocera, D. G.; Stubbe, J. *Biochemistry* **2003**, *42*, 14541. (b) Chang, M. C. Y.; Yee, C. S.; Nocera, D. G.; Stubbe, J. *J. Am. Chem. Soc.* **2004**, *126*, 16702. (c) Seyedsayamdost, M. R.; Stubbe, J. *J. Am. Chem. Soc.* **2006**, *128*, 2522.
- (8) Seyedsayamdost, M. R.; Xie, J.; Chan, C. T.; Schultz, P. G.; Stubbe, J. *J. Am. Chem. Soc.* **2007**, *129*, 15060.
- (9) Yokoyama, K.; Uhlin, U.; Stubbe, J. *J. Am. Chem. Soc.* **2010**, *132*, 8385.
- (10) Yee, C. S.; Chang, M. C. Y.; Ge, J.; Nocera, D. G.; Stubbe, J. *J. Am. Chem. Soc.* **2003**, *125*, 10506.
- (11) Seyedsayamdost, M. R.; Yee, C. S.; Reece, S. Y.; Nocera, D. G.; Stubbe, J. *J. Am. Chem. Soc.* **2006**, *128*, 1562.
- (12) Rappaport, F.; Boussac, A.; Force, D. A.; Peloquin, J.; Brynda, M.; Sugiura, M.; Un, S.; Britt, R. D.; Diner, B. A. *J. Am. Chem. Soc.* **2009**, *131*, 4425.
- (13) Wilkins, B. J.; Marionni, S.; Young, D. D.; Liu, J.; Wang, Y.; Di Salvo, M. L.; Deiters, A.; Cropp, T. A. *Biochemistry* **2010**, *49*, 1557.
- (14) Incorporation of *o*-nitrobenzyl- $F_nY$ s at position 730 of  $\alpha 2$  was previously attempted. The location of this residue in the protein interior resulted in inefficient decaging. Additionally, recovery of protein activity after photolysis was poor, likely as a result of side reactions with neighboring redox-active amino acids.
- (15) Young, T. S.; Schultz, P. G. *J. Biol. Chem.* **2010**, *285*, 11039.
- (16) (a) Xie, J.; Schultz, P. G. *Methods* **2005**, *36*, 227. (b) Liu, C. C.; Schultz, P. G. *Annu. Rev. Biochem.* **2010**, *79*, 413.
- (17) Ge, J.; Yu, G.; Ator, M. A.; Stubbe, J. *Biochemistry* **2003**, *42*, 10071.
- (18) Kobayashi, T.; Nureki, O.; Ishitani, R.; Yaremchuk, A.; Tukalo, M.; Cusack, S.; Sakamoto, K.; Yokoyama, S. *Nat. Struct. Biol.* **2003**, *10*, 425.
- (19) Turner, J. M.; Graziano, J.; Spraggon, G.; Schultz, P. G. *J. Am. Chem. Soc.* **2005**, *127*, 14976.
- (20) (a) Muller, K.; Faeh, C.; Diederich, F. *Science* **2007**, *317*, 1881. (b) Zhou, P.; Zou, J.; Tian, F.; Shang, Z. *J. Chem. Inf. Model.* **2009**, *49*, 2344.
- (21) Young, T. S.; Ahmad, I.; Yin, J. A.; Schultz, P. G. *J. Mol. Biol.* **2010**, *395*, 361.
- (22) (a) Young, D. D.; Young, T. S.; Jahnz, M.; Ahmad, I.; Spraggon, G.; Schultz, P. G. *Biochemistry* **2011**, *50*, 1894. (b) Miyake-Stoner, S. J.; Refakis, C. A.; Hammill, J. T.; Lusic, H.; Hazen, J. L.; Deiters, A.; Mehl, R. A. *Biochemistry* **2010**, *49*, 1667.
- (23) Minnihan, E. C.; Seyedsayamdost, M. R.; Uhlin, U.; Stubbe, J. *J. Am. Chem. Soc.* **2011**, *133*, 9430.
- (24) Yokoyama, K.; Uhlin, U.; Stubbe, J. *J. Am. Chem. Soc.* **2010**, *132*, 15368.
- (25) Yokoyama, K.; Smith, A. A.; Corzilius, B.; Griffin, R. G.; Stubbe, J. Submitted.
- (26) Stoll, S.; Schweiger, A. *J. Magn. Reson.* **2006**, *178*, 42.
- (27) Bollinger, J. M., Jr.; Tong, W. H.; Ravi, N.; Huynh, B. H.; Edmondson, D. E.; Stubbe, J. *Methods Enzymol.* **1995**, *258*, 278.
- (28) Li, C.; Wang, G. F.; Wang, Y.; Creager-Allen, R.; Lutz, E. A.; Sronce, H.; Slade, K. M.; Ruf, R. A.; Mehl, R. A.; Pielak, G. J. *J. Am. Chem. Soc.* **2010**, *132*, 321.